A Versatile Wet-Chemical Method for Synthesis of One-Dimensional Ferric and Other Transition Metal Oxides

Ziyi Zhong,*,† Ming Lin,‡ Vivien Ng,† Gary Xian Boon Ng,† Yonglim Foo,‡ and Aharon Gedanken*,§

Institute of Chemical Engineering and Sciences, 1 Pesek Road, Jurong Island, Singapore 627833, Institute of Materials Research and Engineering, 3 research Linker, Singapore 117602, and Department of Chemistry and Kanbar Laboratory for Nanomaterials, Bar-Ilan University Center for Advanced Materials and Nanotechnology, Bar-Ilan University, Ramat-Gan 52900, Israel

Received August 2, 2006. Revised Manuscript Received September 11, 2006

We developed a versatile method using alkylamines (octylamine and isobutylamine) as structure-directing agents for synthesis of various 1D transition metal oxides in aqueous solution. In this report, 1D iron and copper oxide precursors (for simplicity, we have denoted them as pre-Fe_2O_3 and pre-CuO) and ZnO were prepared. After calcination and reduction, the 1D nanostructure of pre-Fe_2O_3 can be easily converted to 1D α-Fe_2O_3 and 1D Fe_3O_4, successively. The aspect ratio of the 1D nanostructures increases with the reaction time. XRD, TEM, in situ TEM, and TGA were used to characterize the samples. Results showed that after calcination at temperatures higher than 300 °C, the as-prepared 1D pre-Fe_2O_3, which was polycrystalline, transformed into 1D single-crystalline α-Fe_2O_3. A mechanism of assembling and "packing" along a certain direction for the growth of the 1D nanostructure was confirmed.

1. Introduction

In recent years, intensive research efforts have been made to synthesize/fabricate one-dimensional (1D) nanostructured materials (wires, rods, and tubes) because of their unique chemical and physical properties that are different from their bulk counterparts, as well as their potential applications in nanodevice fabrication.[1,2,3] Methods for the synthesis/fabrication of 1D nanostructures include the vapor-phase synthesis (VS) and vapor−liquid−solid (VLS) method, templating against solid porous nanostructures and some wet chemical methods, such as hydrothermal and solvothermal methods,[4] etc. The VS process is suitable for synthesis of 1D metallic materials,[5] whereas the VLS process is mainly used for the production of 1D semiconductor materials with single-crystalline structures.[6] Using templates such as porous alumina is a powerful tool for the synthesis of many 1D materials, but it usually leads to the formation of polycrystalline 1D structures.[7] Furthermore, the residue of the template often contaminates the 1D structures. Some mild solution methods using capping agents such as poly(vivyl pyrrolidone) (PVP) in polyol,[8] amino acid,[9] and glucose[10] for preparation of precious metal wires have also been reported. However, synthesis of 1D transition metal oxides under mild conditions in aqueous solution still poses a big challenge.

Potentially, some organic amines are another type of capping agent that can lead to the formation of 1D transition metal oxides. The first two successful examples are the synthesis of vanadium oxide[11] and $Mg(OH)_2$ nanotubes[12] using hexadecylamine and ethylenediamine as the structure-directing agents, respectively. These breakthroughs opened up a new area for 1D transition metal oxides synthesis. Very recently, we first synthesized 1D and porous TiO_2 using octylamine (denoted as OLA) as a capping agent. The synthesis method was improved by slowing down the hydrolysis process of Ti isopropoxide via coupling with an esterification reaction between isopropanol and acetic acid.[13] It seems there are two key factors that determine whether the 1D nanostructures can be formed: (1) the adsorption of alkylamine molecules on surfaces of the formed particles of the transition metal oxides or their precursors that can cause

* Corresponding author. E-mail: Zhong_ziyi@ices.a-star.edu.sg (Z.Z.); gedanken@mail.biu.ac.il (A.G.).
† Institute of Chemical Engineering and Sciences.
‡ Institute of Materials Research and Engineering.
§ Bar-Ilan University.

(1) Iijima, S. *Nature* **1991**, *354*, 56−58.
(2) Rao, C. N. R.; Deepak, F. L.; Gundiah, G.; Govindaraj, A. *Prog. Solid State Chem.* **2003**, *31*, 5−147.
(3) (a) The Royal Society and The Royal Academy of Engineering Report, *Nanoscience and Nanotechnology*, July 2004, pp 35−50. (b) *Nanochemistry: A Chemical Approach to Nanomaterials*; Ozin, G. A, Arsenault, A. C, Eds.; RSC Publishing: London, 2004; pp 167−259.
(4) Xia, Y.; Yang, P.; Sun, Y.; Wu, Y.; Mayers, B.; Gates, B.; Yin, Y.; Kim, F.; Yan, H. *Adv. Mater.* **2003**, *15* (5), 353−389.
(5) Sears, G. W. *Acta Metall.* **1953**, *1*, 457.
(6) Duan, X.; Lieber, C. M. *Adv. Mater.* **2000**, *12*, 298.
(7) Zhan, J.; Bando, Y.; Hu, J.; Golberg, D.; Kurashima, K. *Small* **2006**, *2* (1), 62−65.
(8) Sun, Y.; Gates, B.; Mayers, B.; Xia, Y. *Nano. Lett.* **2002**, *2*, 165.
(9) (a) Zhong, Z.; Luo, J.; Ang, T. P.; Highfield, J.; Lin, J.; Gedanken, A. *J. Phys. Chem. B* **2004**, *108*, 18119−18123. (b) Zhong, Z.; Patskovskyy, S.; Bouvrette, P.; Luong, J., Gedanken, A. *J. Phys. Chem. B* **2004**, *108*, 4046−4052.
(10) Zhang, J.; Du, J.; Han, B.; Liu, Z.; Jiang, T.; Zhang, Z. *Angew. Chem., Int. Ed.* **2006**, *45*, 1116−1119.
(11) Spahr, M. E.; Bitterli, P.; Nesper, R.; Muller, M.; Krumeich, F.; Nissen, H. U. *Adv. Mater.* **1998**, *10*, 1263−1265.
(12) Li, Y.; Sui, M.; Ding, Y.; Zhang, G.; Zhuang, J.; Wang, C. *Adv. Mater.* **2000**, *12*, 818−821.
(13) (a) Zhong, Z.; Ang, T. P.; Luo, J.; Gan, H. C.; Gedanken, A. *Chem. Mater.* **2005**, *17*, 6814. (b) Zhong, Z.; Chen, F.; Ang, T. P.; Han, Y. F.; Lim, W.; Gedanken, A. *Inorg. Chem.* **2006**, *45*, 4619.

10.1021/cm061821r CCC: $33.50
Published on Web 11/09/2006

a preferential growth or assembling along certain directions, and (2) a slow supply of building blocks of the transition metal oxide precursors or a slow hydrolysis process of the transition metal salts.[13] In other words, the hydrolysis and condensation steps should be well-separated. If not, uncontrolled branching among building blocks by formation of M−O−M (M = transition metals) bonds may occur at many sites or locations, leading to unguided growth. Because the hydrolysis of Ti alkoxides is inherently faster than that of many other transition metal salts, the control on hydrolysis for other transition metal salts should be much easier than that of Ti alkoxides. Naturally, we were concerned about whether the above-mentioned method could be extended to the preparation of other transition metal oxides with 1D nanostructures.

Here, we report the synthesis of 1D α-Fe_2O_3, CuO, and ZnO using octylamine as a structure-directing agent. α-Fe_2O_3 and CuO can be used as catalysts, magnetic materials,[14] and sensors.[15] Wurtzite ZnO has a wide band gap (3.437 eV at 2 K) and is widely used in piezoelectric transducers, varistors, etc.[16] So far, there are only a few examples reported for the synthesis of single-crystalline 1D iron oxides (Fe_3O_4 and Fe_2O_3) under mild aqueous conditions, e.g., the synthesis of single-crystalline α-Fe_2O_3 nanotubes by reacting $FeCl_3$ with $NH_4H_2PO_4$ under hydrothermal conditions, sol−gel-mediated synthesis of Fe_2O_3 in reverse micelles, and magnetic-field-induced growth of single-crystalline Fe_3O_4 nanowires.[17] Interestingly, in our case, the as-synthesized 1D Pre-Fe_2O_3 is polycrystalline but can be converted to single-crystalline α-Fe_2O_3 nanorods after being annealed above 300 °C. After further reduction, the nanorods can be converted to 1D Fe_3O_4. The aspect ratio of these 1D nanostructures can reach the range of 10−20. The same strategy is also applicable to the synthesis of 1D CuO, ZnO, and TiO_2. Therefore, this report presents a new general method for synthesizing novel 1D transition metal oxides. In addition, we provide herein strong evidence supporting the assembling and packing mechanism for the formation of the 1D nanostructures.

2. Experimental Section

All chemicals were purchased from Aldrich and used as received. In a typical synthesis, 1.0 g of $Fe(NO_3)_3 \cdot 9H_2O$ was dissolved in 10 mL of distilled water (DI H_2O), and then a certain quantity of octylamine and 1.5 g of urea were added to the vessel. The mixture was stirred for several minutes and transferred into a screw-capped autoclave lined with a Teflon vessel. Finally, the autoclave was put in an oven with a temperature setting of 80 °C for 7 h. After the reaction, the precipitate was washed four times with acetone or anhydrous ethanol and dried in a vacuum oven at 100 °C.

The morphology and size of the products were observed employing a transmission electron microscope (TEM, Tecai TF20 Super Twin, 200kV). In situ TEM measurementa were performed on a JEOL 2000 V ultrahigh vacuum TEM (base pressure ≈ 1×10^{-9} Torr). The pre-Fe_2O_3 product was ultrasonically dispersed in pure ethanol and then deposited on a holey carbon-coated Mo grid that was then mounted over a Si heating piece. The specimen was heated from room temperature to higher temperatures step by step. After each temperature setting had been reached for ca. 20 min, TEM images were recorded using a Gatan DV300 image acquisition system, allowing real-time observations of the annealing process. The powder XRD analysis was conducted on a Bruker D8 Advance X-ray diffractometer with $CuK_{\alpha 1}$ radiation, whereas the thermal analysis (TGA) was performed on a SDT 2960 instrument in air flow. Infrared spectra for dried samples were recorded employing a Bio-Rad Excalibur spectrometer by a KBr disc method.

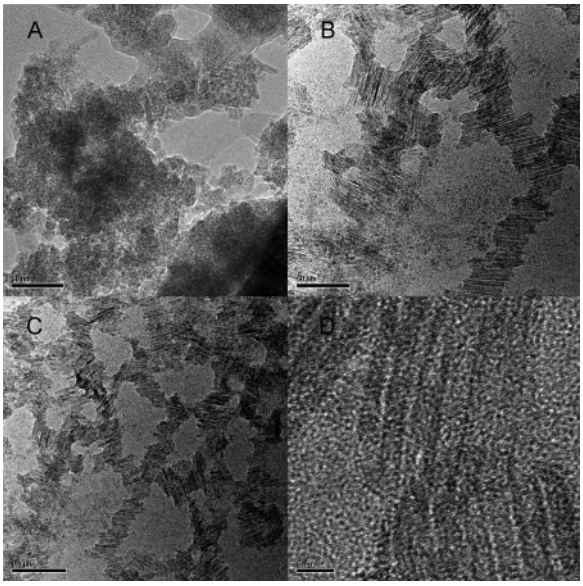

Figure 1. Influence of the OLA/Fe molar ratio on morphology of the pre-Fe_2O_3 product: (A) OLA/Fe = 0.0/1.0, (B) 1.2:1.0, (C, D) 2.4:1.0. The reaction temperature and time were 80 °C and 7 h.

3. Results and Discussion

Figure 1 shows the TEM images of the pre-Fe_2O_3 product prepared at various OLA/Fe molar ratios. When OLA/Fe is 0:1.0, pre-Fe_2O_3 particles with featureless morphology are observed (Figure 1A). An increase in OLA/Fe to greater than 0.5:1 leads to the formation of many pre-Fe_2O_3 nanorods (Figure 1B). The 1D nanostructure estimated by TEM observation accounts for ca. 70−80% of the pre-Fe_2O_3 product. A further increase in the OLA/Fe molar ratio has almost no influence on the morphology and dimensions of the pre-Fe_2O_3 product (images C and D of Figure 1). As observed in TEM, these as-prepared 1-D pre-Fe_2O_3 structures are aligned very well and packed closely (images B and C of Figure 1) because of the hydrophobic attraction among the pre-Fe_2O_3 nanorods that are covered with the OLA molecules on surfaces. To investigate the influence of the OLA molecules and the importance of a slow hydrolysis on the morphology of the pre-Fe_2O_3 product, we conducted two comparison experiments. In the first one, the reaction was conducted without the addition of OLA and urea. As a result,

(14) (a) Brown, A. C. S.; Hargreeaves, J. S. J. Rijnierse, B. *Catal. Lett.* **1998**, *53*, 7. (b) Landon, P.; Ferguson, J.; Solsona, B. E.; Garcia, T.; Garley, A. F.; Herzing, A. A.; Kieley, C. J.; Golunski, S. E.; Hutching, C. J. *Chem. Commun.* **2005**, 3385. (c) Pillai, U. R.; Deevi, S. *Appl. Catal., B* **2006**, *64*, 146−151. (d) Klabunde, K. J.; Zhang, D.; Glavee, G. N.; Sorensen, C. M. *Chem. Mater.* **1994**, *6*, 784.

(15) Sun, H. T.; Cantalini, C.; Faccio, M.; Pelino, M.; Catalano, M.; Hapfer, L. *J. Am. Ceram. Soc.* **1996**, *79*, 927.

(16) (a) Ip, K.; Heo, Y. W.; Baik, K. H.; Norton, D. P.; Pearton, S. J.; Kim, S.; LaRoche, J. R.; Ren, F. *Appl. Phys. Lett.* **2004**, *84*, 2835. (b) Carlens, C. L.; Klabunde, K. J. *Langmuir* **2000**, *16*, 3764−3772.

(17) (a) Xia, C. J.; Sun, L. D.; Yan, Z. J.; You, L. P.; Luo, F.; Han, X. D.; Pang, Y. C.; Zhang, Z.; Yan, C. H. *Angew. Chem., Int. Ed.* **2005**, *44*, 4328−4333. (b) Woo, K.; Lee, H. J.; Ahn, J. P.; Park, Y. S. *Adv. Mater.* **2003**, *15*, 1761−1764. (c) Wang, J.; Chen, Q.; Zeng, C.; Hou, B. *Adv. Mater.* **2004**, *16*, 137−140.

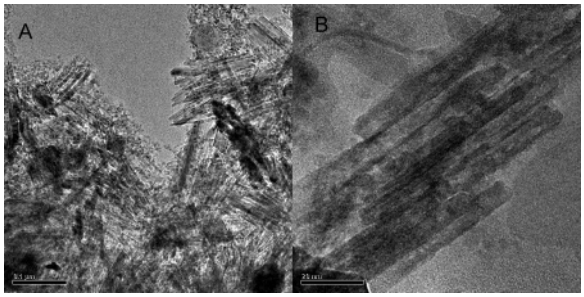

Figure 2. Influence of the reaction time on the length of the 1D pre-Fe_2O_3. The reaction conditions are the same as that in images C and D of Figure 1 except the reaction time was increased from 7 to 70 h. (A, B) TEM images at low and high magnification, respectively.

only olive-shaped pre-Fe_2O_3 particles with a size of ca. 200 nm were obtained (see the Supporting Information, Figure SI-1). In the second one, NaOH was used to replace urea, and no 1D pre-Fe_2O_3 nanostructure was formed, even in the presence of OLA. In the second experiment, the formation of the pre-Fe_2O_3 particles was so fast that these small particles aggregated immediately, thus losing control over the growth direction. This impact of growth kinetics on morphology was also observed in the case of TiO_2.[13b]

The aspect ratio of the 1D pre-Fe_2O_3 is determined by the reaction time. Figure 2 shows the TEM image of the pre-Fe_2O_3 product with a reaction time as long as 70 h. The dimension of the 1D structure in cross-section is ca. 4−5 nm and does not change with the reaction conditions (Figures 1D and Figure 2B). However, the length of the 1D structure of the pre-Fe_2O_3 product increased to 100−120 nm (images A and B of Figure 2) from previous 50−60 nm (Figure 1B−D). This increase in the aspect ratio with the reaction time is due to the increase in the length of the 1D nanostructure, rather than the change of the dimensions in the cross-section. The longer the reaction time, the higher the aspect ratio.

The reaction temperature also influences the final morphology of the pre-Fe_2O_3 product. After conducting the reaction at 60 °C for 5 h, only small pre-Fe_2O_3 particles were obtained (see the Supporting Information, Figure SI-3A). When the reaction temperature was increased to above 70 °C, a 1D structure was obtained (see the Supporting Information, Figure SI-3B). With the further increase in the reaction temperature to 120 °C, the formed pre-Fe_2O_3 product is better crystallized but no change in morphology is observed. Electronic diffraction (ED) on the pre-Fe_2O_3 rods confirmed that the as-prepared pre-Fe_2O_3 was composed of polycrystallites (see the Supporting Information, Figure SI-2B). Although it looks as though there is no sign of crystalline structure from HRTEM (Figure 1D), ED is a more convincible tool for confirming whether the structure is amorphous or crystalline.

The 1D structure of pre-Fe_2O_3 can be further converted to 1D α-Fe_2O_3 and 1D Fe_3O_4 by simple calcination and reduction at high temperatures. Images A and B of Figure 3 show the 1D pre-Fe_2O_3 nanostructure calcined at 300 °C in air. The contrast of these TEM images is much better than that of the TEM images shown in Figure 1 and 2, because of an improved crystallinity. Upon closer observation with high-resolution TEM (Figure 3B), it was found that single-crystalline of 1D α-Fe_2O_3 formed after calcination at 300

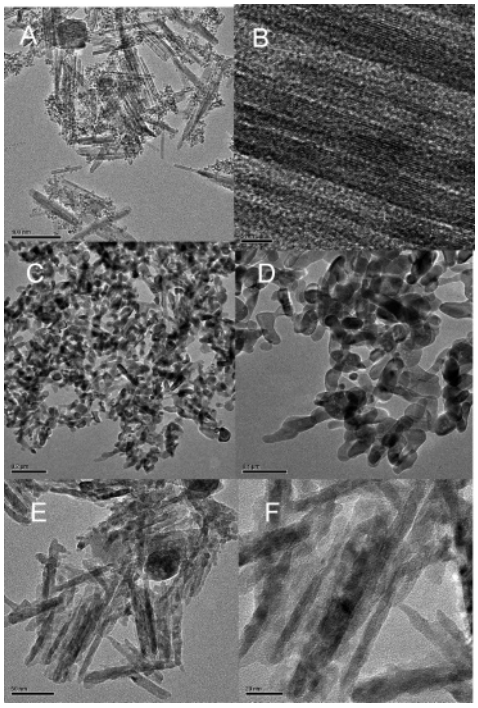

Figure 3. Stability of the 1D nanostructure of pre-Fe_2O_3 and α-Fe_2O_3: the 1D pre-Fe_2O_3 was calcined at (A) 200, (B) 300, (C) 550, and (D) 600 °C, respectively. The iron oxide sample was prepared using octylamine as a structure-directing agent. The reaction temperature and time were 80 °C and 50 h, and the OLA/Fe molar ratio was 2.4:1. (E, F) Fe_3O_4 particles formed by reducing the α-Fe_2O_3 shown in B at 300 °C in 5% H_2.

°C. When the calcination temperature was increased to above 550 °C, most of the α-Fe_2O_3 nanorods collapsed into shorter nanorods and the particles became irregularly shaped (Figure 3C). Above 600 °C, no 1D nanostructure of α-Fe_2O_3 nanoparticles was observed (Figure 3D). The thermal stability of the 1D structure against calcination was also monitored by in situ TEM measurement, in which bright-field (BF) and dark-field (DF) TEM images for three selected areas of the 1D structure at 10 different temperatures were recorded; some of these results are shown in Figure 4. At room temperature, the chosen pre-Fe_2O_3 nanorod (see the cycle in the DF image in Figure 4 recorded at RT) was composed of small bright dots, verifying the polycrystalline nature of the nanorod. After calcination at 320 and 420 °C, these bright dots gradually emerged into a uniform bright rod, revealing the formation of single-crystalline 1D α-Fe_2O_3. After calcination at 550 °C, the bright rod disappeared again because of the collapse of the 1D α-Fe_2O_3 (see the TEM images taken at various temperatures for the nanorod in the cycle). Similar changes with temperature can be seen for other pre-Fe_2O_3 nanorods. After the in situ TEM measurement, one electronic diffraction pattern was recorded for one chosen α-Fe_2O_3 nanorod (the nanorod inset in Figure 5). It shows that the 1D α-Fe_2O_3 was single crystalline and that its growth direction is along $[2\bar{1}0]$, which is in agreement with the result of the conventional TEM observation (Figure 3B). The X-rays diffraction experiment showed that the as-prepared 1D pre-Fe_2O_3 is amorphous (Figure 6C, bottom line), but after calcination at 300 °C, reflections of the α-Fe_2O_3 appeared (Figure 6C, middle line, compared with the top line, which is for α-Fe_2O_3 from Aldrich; the lines match well with the JCPDS 01-089-8103 of α-Fe_2O_3 and that of the

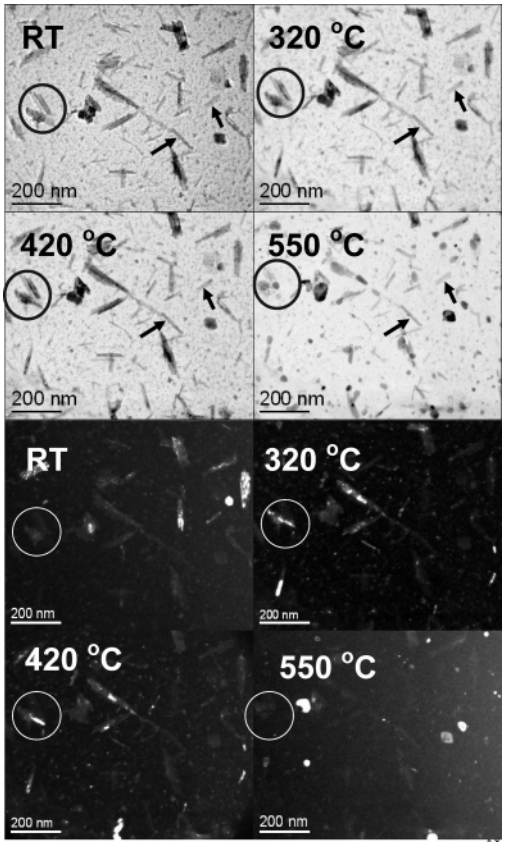

Figure 4. In situ TEM images of 1D pre-Fe_2O_3 calcined at various temperatures. Shown in upper half of the figre are bright-field images taken at different temperatures, and in the lower half are their corresponding black-field images.

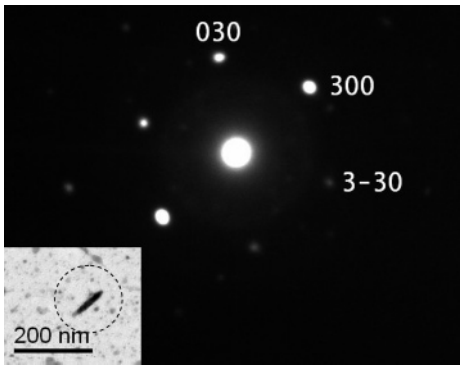

Figure 5. Electron diffraction pattern of 1D α-Fe_2O_3 formed after the in situ TEM measurement at 550 °C. Single crystalline α-Fe_2O_3 was formed and the growth direction of the α-Fe_2O_3 is along [$2\bar{1}0$].

commercial α-Fe_2O_3 from Aldrich). The 1D pre-Fe_2O_3 transformed directly to the α-Fe_2O_3 phase, and no indication for an intermediate γ-Fe_2O_3 phase was observed.

The as-prepared 1D pre-Fe_2O_3 was in its precursor form and contained copious amounts of H_2O and OLA molecules. From the TGA measurement (Figure 6A), the total weight loss was ca. 53% after the calcination at 300 °C. As indicated by XRD result, α-Fe_2O_3 was formed above this temperature. Assuming that $Fe(OH)_3$ or FeO(OH) was the 1D pre-Fe_2O_3 and that the final product was α-Fe_2O_3, the calculated weight losses would be 24.8 and 10.1%, respectively, much lower than the 53% that we observed. The "packing" of the rodlike micelle structures or the assembly should exist in the 1D pre-Fe_2O_3 even after being washed thoroughly with acetone or ethanol. The derivative weight curve exhibits a sharp peak at 215 °C, revealing that the pre-Fe_2O_3 was decomposed near this temperature. These results are confirmed by FTIR measurements for the pre-Fe_2O_3 samples treated at different temperatures, and for comparison, the IR spectrum of the liquid octylamine (OLA; Figure 6B). In the spectra, bands at 2926 and 2845 cm^{-1} are assigned to C−H vibrations, and the bands at 3367, 3290, and 1606 cm^{-1} are assigned to N−H vibrations.[18] These main C−H and N−H vibration bands are marked by dotted and dashed lines, respectively, in Figure 6B. Clearly, the C−H and N−H vibrations are seen even when the sample was treated at 200 °C, indicating that the OLA molecules were not removed even after being washed with acetone and ethanol or calcined at 200 °C. Most likely, there is chemical or hydrogen bonding between the OLA molecules and the iron oxide particles,[19] similar to the TiO_2 case in which the amine adducts were formed.[20] The detailed structure of this iron oxide precursor still needs to be clarified in the future. However, after being heated at 250 and 300 °C, all OLA molecules were eliminated, as evidenced by the disappearance of all the C−H and N−H bands. Instead, two bands appear at 1635 and 3414 cm^{-1}, which can be assigned to the absorbed H_2O.[18a] So, the IR results confirm that pre-Fe_2O_3 was converted to α-Fe_2O_3 near 300 °C.

To make sure all water and OLA molecules were removed before reduction for the TPR experiment, we treated the sample at 300 °C (see the Supporting Information, Figure SI-4). The sample was first cooled to room temperature and then reduced with 5% H_2 from room temperature to 375 °C. The TPR curve is shown in Figure SI-4 of the Supporting Information. A sharp H_2-consumption peak was observed at 270 °C, indicating that α-Fe_2O_3 was reduced into Fe_3O_4 before 300 °C. Therefore, in another separate experiment, we reduced the sample shown in Figure 3B with 5% H_2 gas at 300 °C for 1 h. The TEM images of the reduced sample are shown in images E and F of Figure 3. The 1D morphology is still preserved even in the produced Fe_3O_4. But different from the 1D α-Fe_2O_3, the Fe_3O_4 nanostructure has a pearl-necklace pattern. Also, some pores can be discerned in the 1D Fe_3O_4 nanostructure.

The same strategy was extended to the synthesis of CuO and ZnO systems, and 1D nanostructures were also obtained. TEM and SEM images of 1D pre-CuO and ZnO are shown in images A and B of Figure 7, respectively. A bamboolike structure is observed in the pre-CuO case. These pre-CuO nanorods were converted to 1D CuO after heat treatment at 300 °C. Different from the α-Fe_2O_3 and CuO cases, single-crystalline Wurtzite ZnO was formed (the XRD pattern is not shown here, but the pattern matches well with JCPDS-IC-361451), probably because the zinc hydroxide is not stable and ZnO is very easily crystallized. Also, when isobutylamine was used as a capping agent, similar results were observed (TEM images are not shown here). Thus, this

(18) (a) Socrates, G. *Infrared Characteristic Group Frequencies*, 2nd ed.; Wiley & Sons: New York, 1994; pp 74−79. (b) Thimmaiah, S.; Rajamathi, M., Singh, N.; Bera, P.; Meldrum F.; Chandrasekhar, N.; Seshadri, R. *J. Mater. Chem.* **2001**, *11*, 3215.
(19) Li, Y.; Afzaal, M.; O'Brien, P. *J. Mater. Chem.* **2006**, *16*, 2175.
(20) Fric, H.; Schubert, U. *New. J. Chem.* **2005**, *29*, 232.

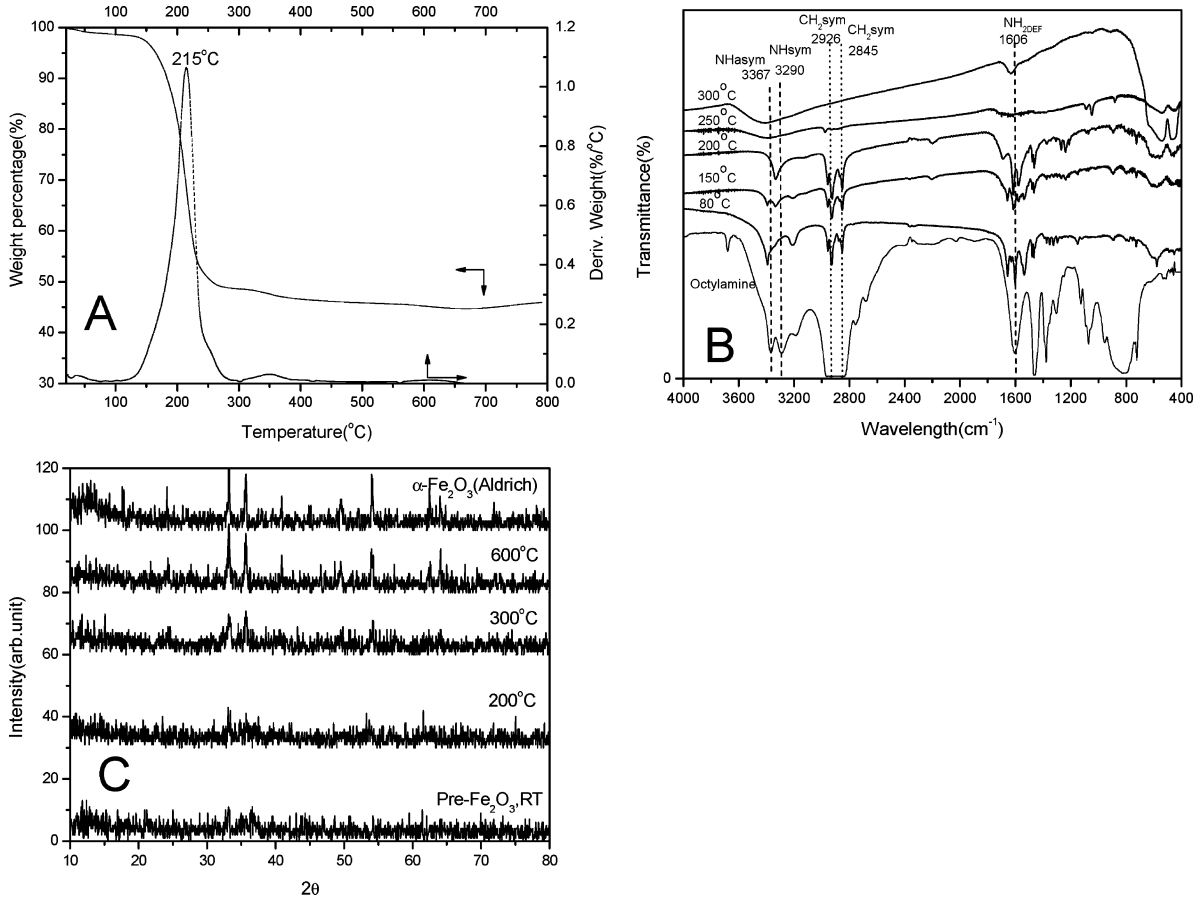

Figure 6. (A) TGA result for the pre-Fe_2O_3 product that was present in Figure 2. (B) IR spectra for the pre-Fe_2O_3 product that was calcined at various temperatures. (C) XRD patterns of the calcined samples at various temperatures. The standard octylamine (IR spectrum) and α-Fe_2O_3 were purchased from Aldrich.

method is versatile for the synthesis of various 1D transition metal oxides.

The formation mechanism of the pre-Fe_2O_3 is a process of assembling and then packing small particles along a certain direction, which was first proposed in our previous studies.[13] In this study, several important pieces of experimental evidence are found that support this mechanism: (1) the length or the aspect ratio of 1D pre-Fe_2O_3 increased with the reaction time, even the pre-Fe_2O_3 product had a constant weight after 5 h of reaction (the hydrolysis of $Fe(NO_3)_3$ was complete after 5 h reaction at 80 °C). In other words, the growth of the 1D pre-Fe_2O_3 is due to assembling of the small pre-Fe_2O_3 particles. Indeed, at a lower reaction temperature (see the Supporting Information, Figure SI-3), or in a shorter reaction time, the TEM results showed that there were more small particles in the pre-Fe_2O_3 product; this also excludes the possibility that the 1D structure is formed via the formation of 1D micelles in the solution. (2) the as-prepared 1D pre-Fe_2O_3 was X-ray amorphous, but its polycrystalline nature was revealed by electronic diffraction (see the Supporting Information, Figure SI-2), showing that these 1D pre-Fe_2O_3 nanostructures were composed of many small crystallites. (3) Pearl-necklace Fe_3O_4 was obtained after reduction with 5% H_2 (images E and F of Figure 3). More clearly, in the case of 1D pre-CuO (Figure 7A), the 1D bamboolike structure made of small particles is verified. (4) Another key factor for the formation of the 1D structure is the slow supply of small pre-Fe_2O_3 particles. When NaOH

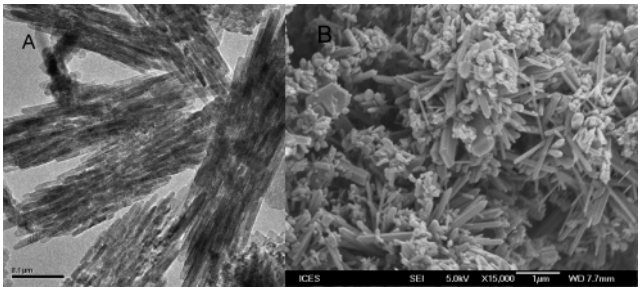

Figure 7. One-dimensional (A) pre-CuO and (B) ZnO, prepared using OLA as the structure-directing agent and Cu acetate and Zn acetate as precursors, respectively. The molar ratio of OLA/Cu or Zn = 1.2:1, and the reaction was conducted at 80 °C for 20 h.

was used to replace urea, no 1D structure was observed because the small pre-pre-Fe_2O_3 particles were formed very fast. As a result, these small particles aggregated into big particles even before the OLA molecules could cover their surfaces well. This principle is well-proven in the TiO_2 case.[13] To the best of our knowledge, this unidirectional packing or assembling mechanism is different from many other cases, e.g., some organic molecules adsorb on some crystal facts of metal particles and lead to the oriented growth along a certain direction by homogeneous nucleation.[4]

Our FTIR and TGA results confirm that OLA molecules exist in the pre-Fe_2O_3 product. The TEM observations suggest that these OLA molecules are anchored on the surface of pre-Fe_2O_3 particles, because we observed that all the as-prepared 1D pre-Fe_2O_3 and pre-CuO nanostructures

are packed in a parallel manner. When the amino groups in the alkylamine molecules are bound to the metal oxide particles, their hydrocarbon tails will stretch out from the surface, causing the particle surfaces to become hydrophobic. As a result, the 1D metal oxide structure will prefer to bundle together because of this hydrophobic interaction.

However, in our case, it is still not very clear why the organic amine molecules can lead to the unidirectional growth of the above-mentioned metal oxides or their precursors. Cozzoli et al.[21] reported that shape control over TiO_2 nanoparticles can be achieved by capping the TiO_2 particles with oleic acid molecules and manipulating their growth kinetics. Sugimoto et al. developed a two-step sol−gel process for synthesis of ellipsoid and cube forms of TiO_2, in which ammonia acted as a shape controller in the aging stage.[22,23] Another example is lysine molecules that possess amino groups and can initiate linear aggregation of Au colloids when capped on Au colloids.[9] Given the fact that the small particles have a high surface energy and are not stable, they always intend to aggregate together. But in our case, because organic amine molecules cover the particle surfaces or certain crystal facets, they will probably impose some restriction on the direction of the particle aggregation. Once two particles are sufficiently close to each other, they can form a joint (or M−O−M bond between two particles; M = transition metals) at one end by shifting some organic molecules away from this end (Scheme 1(1)). This may also occur at one crystal facet that has a lower density of the adsorbed amine molecules. To reduce expulsion or avoid collision among the amine molecules on different small particles, we prefer further linking of a third or more particles to proceed in a linear way (Scheme 1 (2 and 3)). Of course, this happens only when the particle surfaces are covered with a high density of the amine molecules. Otherwise, when the density of the amine molecules or amine/M is low, no control on the direction of the aggregation will be obtained, as the particles may bind to each other anywhere. The hydrothermal treatment probably provides proper conditions such as energy for reorganizing the surfaces of the small particles, for assembling and crystallizing them in the assemblages. However, so far, we still cannot exclude the possibility that the so-called small particles can be some crystallites of some amine-containing complexes, which will be clarified in the future.

4. Conclusions

In conclusion, we have prepared one-dimensional pre-Fe_2O_3, pre-CuO, and ZnO nanostructures using organic amines as the capping agent by a low-temperature, soft-chemical method. The 1D pre-Fe_2O_3 can be easily converted to 1D α-Fe_2O_3 and 1D Fe_3O_4 after calcination and reduction in H_2. The aspect ratio of the 1D pre-Fe_2O_3 and pre-CuO can be tuned by varying the reaction time. The formation of these 1D nanostructures is via an assembling and then packing of small precursor particles (pre-Fe_2O_3, pre-CuO) in an oriented direction. This mechanism for the formation of 1D metal oxides is different from many others given in the literature.[4] This versatile approach can be used for the synthesis of various 1D transition metal oxides and can definitely be scaled up readily.

Scheme 1. Proposed Formation Process for the 1D Transition Metal Oxides

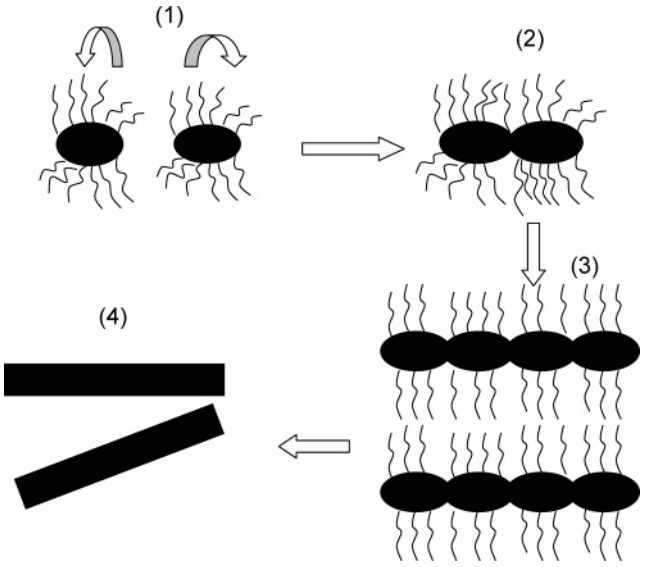

(1) The precursor MO_x particles are covered with amine molecules on the surface, and the OLA molecules tend to move to the middle of the particles so as to empty the ends of the particles, or some crystal facets do have fewer amine molecules. (2) Two particles covered with amine molecules form a joint (M−O−M bonds) at one of their ends or at the crystal facet with fewer amine molecules. (3) The particles covered with amine molecules assemble and pack in a linear formation, leading to the growth of the 1D nanostructures; the hydrophobic interaction among the 1D nanostructures force them to pack in a parallel way, as observed in TEM measurement. The amine molecules prevent the linear structure from collapsing. (4) After the amine molecules on the surface are eliminated and further crystallization takes place, 1D MO_x nanostructures are formed.

Acknowledgment. This collaborative research was supported by the Agency for Science, Technology and Research in Singapore (A-STAR, ICES04-414001). Z.Z. thanks Dr. Siew Pheng Teh, Jie Bu, and Ms. Jaclyn Teo for technical assistance and helpful discussions, and Dr. Keith Carpenter and Dr. P. K. Wong for their support to this project.

Supporting Information Available: Images from the comparison experiments; plot of the temperature-programmed reduction of the 1D pre-Fe_2O_3 product (PDF). This material is available free of charge via the Internet at http://pubs.acs.org.

CM061821R

(21) Cozzoli, P. D.; Kornowski, A.; Weller, H. *J. Am. Chem. Soc.* **2003**, *125*, 14539.
(22) (a) Chemseddine, A.; Moritz, T. *Eur. J. Inorg. Chem.* **1999,** 235. (b) Kanie, K.; Sugimoto, T. *Chem. Commun.* **2004**, 1584. (c) Sugimoto, T.; Okada, K.; Itoh, H. *J. Colloid Interface Sci.* **1997**, 193.
(23) (a) Li, Y.; Sui, M.; Ding, Y.; Zhang, G.; Zhuang, J.; Wang, C. *Adv. Mater.* **2000**, *12*, 818. (b) Muhr, H. J.; Krumeich, F.; Schonholzer, U. P.; Bieri, F.; Niederberger, M.; Gauckler, L. J.; Nesper, R. *Adv. Mater.* **2000**, *12* (3), 231.